Original Paper

Cells Tissues Organs

Cells Tissues Organs
DOI: 10.1159/000441053

Accepted after revision: September 10, 2015
Published online: November 13, 2015

Three-Dimensional Platelet-Rich Plasma Hydrogel Model to Study Early Tendon Healing

Eva Rubio-Azpeitia[a] Pello Sánchez[b] Diego Delgado[b] Isabel Andia[a]

[a]BioCruces Health Research Institute, Cruces University Hospital, Barakaldo, and [b]Arthroscopic Surgery Unit Research, Hospital Vithas San José, Vitoria-Gasteiz, Spain

Key Words

Platelet-rich plasma · Tendon · Cell culture · Extracellular matrix · Angiogenesis · Inflammation

Abstract

Since the experimental conditions of cell cultures may bias results, it is critical to use suitable models. This is also true in the context of tendon cell biology and the study of platelet-rich plasma (PRP) therapies and PRP-augmented cell-based therapies. We compared the culture of human tendon cells in 2 dimensions (2D) with PRP-supplemented media to culture in matching 3-dimensional (3D) PRP hydrogels. Cell proliferation, cell shape, and the pattern of gene and protein expression were examined. Our data revealed modifications in cell shape and enhanced expression of tenomodulin and scleraxis in 3D hydrogels. Additionally, protein secretion analysis using glass-based arrays specific for angiogenesis revealed differences in interleukin (IL)-6 and IL-8 protein expression between 2D cultures and 3D hydrogels, while the secretion of other angiogenic or inflammatory cytokines was unaffected. Our study suggests that 3D hydrogels are physiologically more relevant than 2D cultures in the study of tendon cells, based on cell shape, support of tenocyte proliferation, phenotype, and the pattern of gene and protein expression.

Introduction

The tendon lacks intrinsic healing resources. Endogenous healing barriers are attributed to low cellularity, scarce vascularity, and the absence of nerves. Therefore, microinjuries induced by repetitive loading often progress to tendon degeneration. To overcome these healing deficits, several biological strategies, including the use of recombinant growth factors [Lamplot et al., 2014; Kovacevic et al., 2015], are being explored. Alternatively, the use of a physiological pool of growth factors and cytokines may change the otherwise flat tendon response in the initial stages of healing [Andia et al., 2010].

In this context, platelet-rich plasma (PRP) is used to overcome the endogenous limitations of tendon repair. Several in vitro tendon models have been developed with the aim of elucidating the potential of PRP therapies. In fact, PRP research is eminently translational, and current PRP-based clinical applications rely on existing experimental data.

An insufficient number of cells and inadequate synthesis of extracellular matrix (ECM) molecules are critical impediments for tendon healing. Tendon cells exposed to PRP show enhanced proliferation and synthesis of ECM molecules [Anitua et al., 2007]. Moreover, tendon cells respond to PRP by synthesizing modulators of inflamma-

KARGER

E-Mail karger@karger.com
www.karger.com/cto

1422–6405/15/0000–0000$39.50/0

Isabel Andia, PhD
Regenerative Medicine Laboratory, BioCruces Health Research Institute
Cruces University Hospital, Pza Cruces s/n
ES–48903 Barakaldo (Spain)
E-Mail iandia2010@hotmail.com

Abbreviations used in this paper

2D	2-dimensional
3D	3-dimensional
ACAN	aggrecan
COL1A1	type 1 collagen
COL3A1	type 3 collagen
COMP	cartilage oligomeric matrix protein
DCN	decorin
DMEM	Dulbecco's modified Eagle's medium
ECM	extracellular matrix
FBS	fetal bovine serum
FMOD	fibromodulin
FN	fibronectin
GAPDH	glyceraldehyde-3-phosphate dehydrogenase
HA	hyaluronan
HAS2	hyaluronan synthase 2
IL	interleukin
MKX	Mohawk homeobox
OD	optical density
PRP	platelet-rich plasma
RT	room temperature
SCX	scleraxis
TBP	TATA-box-binding protein
TNMD	tenomodulin
VCAN	versican
VEGF	vascular endothelial growth factor
XTT	2,3-bis(2-methoxy-4-nitro-5-sulfophenyl)-5-[(phenylamino) carbonyl]-2H-tetrazolium hydroxide

tion and angiogenesis with paracrine effects on endothelial and innate immune cells [Andia et al., 2015]. This information, obtained from 2-dimensional (2D) cultures exposed to PRP supernatants or lysates, constitutes the starting point for further experimental research. However, there are increasing concerns regarding whether this culture system is physiologically relevant to tendon biology [Spanoudes et al., 2014].

To address this issue, we devised a 3-dimensional (3D) PRP hydrogel culture technique that allows us to study tendon cell biology in a model halfway between conventional in vitro cultures and tissue engineering constructs in 3D fibrin matrices [Bayer et al., 2014]. Evidently, PRP hydrogels do not intend to emulate the highly organized ECM of native tendons, but the data obtained here can help to better understand the effects of PRP in a more physiological 3D spatial context and in a molecular environment that mimics early healing. The fibrin matrix obtained from PRP is a natural hydrogel that originates in the polymerization of the plasmatic fibrinogen, which occurs when anticoagulated plasma is in the presence of Ca^{2+}, a necessary cofactor for the transformation of plasma prothrombin into thrombin. The latter cleaves fibrinopeptides and converts soluble fibrinogen into the insoluble fibrin network that has a high density of covalent crosslinks. Fibronectin (FN), vitronectin, osteonectin, and α_2-plasmin inhibitor, as well as other plasmatic proteins, are naturally incorporated into fibrin during coagulation by a specific crosslinking reaction mediated by factor XIIIa. Additionally, molecular signals are naturally incorporated into the gel [Nurden et al., 2008] and participate in tendon healing along with coagulation and complement factors [Cazander et al., 2012; Hammerman et al., 2014].

The purpose of this study is to compare 2 cell culture models to assess the influences of biophysical and molecular signals contained in PRP on tendon cell biology. A conventional 2D cell culture model using liquid PRP as the medium supplement was compared with cells cultured in 3D PRP hydrogels.

Materials and Methods

Tenocyte Isolation

Human tendon samples were obtained from 2 young healthy males during anterior cruciate ligament reconstruction surgery with the semitendinosus tendon. The local Ethics Committee approved this study, and written informed consent was obtained from all donors. Tendon cells were isolated as previously described [Andia et al., 2014b] and expanded using 10% fetal bovine serum (FBS; Hyclone; GE Healthcare, Cleveland, Ohio, USA) until passage 2 and passage 10 were reached. Cells were starved for 24 h in T75 flasks (Corning, New York, N.Y., USA), harvested after trypsinization (TrypLE Select; Gibco, Life Technologies, USA), and seeded at a concentration of 4×10^4 cells/well in 6-well plates and treated with PRP as described below. Experiments were performed at passage 2 and passage 10.

PRP Preparation

PRP was prepared from the peripheral blood of 4 healthy donors (2 males and 2 females, n = 4). Briefly, 9 ml of peripheral blood was withdrawn using citrate as the anticoagulant and centrifuged at 570 *g* for 7 min to separate the PRP from the buffy coat and red blood cells. This PRP contained a moderate concentration of platelets (platelet fold increase of 2.25, SE 0.26) and no leukocytes. The PRP lysate for cell cultures was prepared in 3 successive freeze/thaw cycles followed by sterile filtration over 0.22-μm syringe filters (Millipore, Darmstadt, Germany). Aliquots were stored at –20°C.

Proliferation Assays in 2D Cultures and 3D PRP Hydrogels

The tendon cells were loaded at a density of 4,000 cells/well in 3D PRP hydrogels prepared from 4 donors. In parallel, cells were seeded at a density of 4,000 cells/well in 96-well plates and treated with 10% PRP lysate from 4 donors. As a reference, cells were cultured with 10% FBS. Cell proliferation was assayed at 0, 24, 48, 72, and 96 h using 2,3-bis(2-methoxy-4-nitro-5-sulfophenyl)-5-[(phenylamino) carbonyl]-2H-tetrazolium hydroxide (XTT),

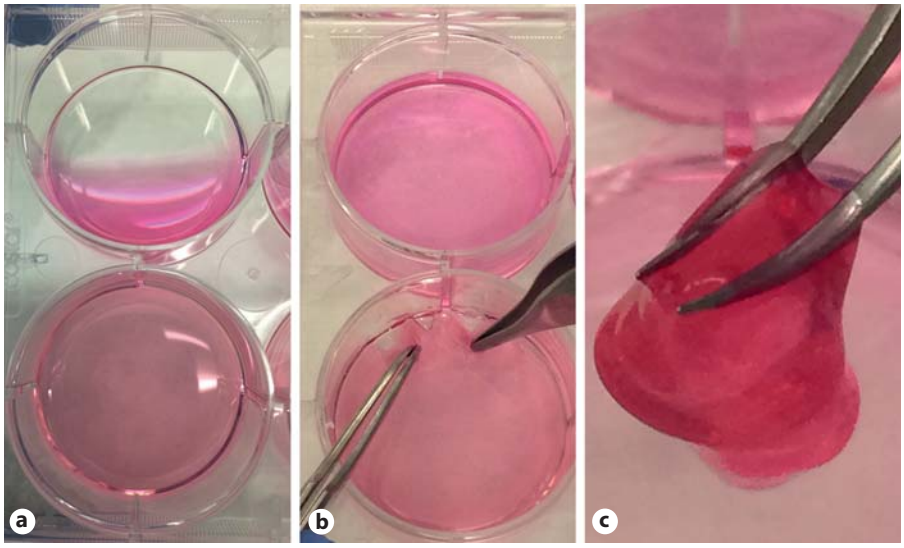

Fig. 1. Macroscopic illustration of PRP hydrogel formation. **a** The upper well shows DMEM supplemented with 10% PRP lysate treated with heparin, and the lower well shows DMEM supplemented with 10% PRP lysate. **b** After 30 min of incubation at 37°C, a translucent hydrogel is formed in the lower well. **c** Visualization of cells embedded in PRP hydrogel is straightforward because of gel transparency.

which only detects metabolically active cells (Cell Proliferation Kit II; Roche, Basel, Switzerland).

2D and 3D Cultures

For 2D cultures, cells were seeded into 6-well plates (Corning) at a concentration of 4×10^4 cells/well and cultured with Dulbecco's modified Eagle's medium (DMEM) F12 (Gibco, Life Technologies) supplemented with 10% PRP lysate and 1 U/ml heparin (Hospira 5%; Lake Forest, Ill., USA).

For 3D PRP hydrogel culture, cells were resuspended in culture medium with 10% PRP lysate at a density of 4×10^4 cells/well in 6-well plates. The presence of Ca^{2+} in the culture medium (1.05 mM) induces thrombin formation and the subsequent cleavage of fibrinogen and polymerization of fibrin dimers. Upon fibrin formation, tendon cells are captured within the hydrogel. Fibrin polymerization occurs 20–30 min after setting of the mixture (cells, media, and PRP) at 37°C (fig. 1). We set up 3 technical replicates of 8 independent cultures for gene expression and protein assessments. In addition, cell metabolism was assessed at 96 h for each cell donor/PRP donor using the XTT assay. Cells were cultured in these conditions for 4 days. Thereafter, PRP hydrogels were centrifuged to harvest the aqueous phase. Likewise, the supernatants of the 2D cultures were harvested after 4 days of cultivation and served as controls for the 3D conditions. In parallel, cells were harvested for RNA isolation. Hydrogels were stable during the 4-day cultivation period (we did not add any fibrin stabilizer, e.g. tranexamic acid).

Cell Morphology Analysis by Immunocytochemistry

Cells were seeded in a sterile µ-Dish$^{35\ mm,\ high}$ (IBIDI, GmbH, Germany) in DMEM F12 mixed with 10% PRP which was allowed to clot directly in the dish. After 96 h, the cells were fixed with a 10% neutral buffered formalin solution (Sigma-Aldrich, St. Louis, Mo., USA) for 15 min and washed twice with PBS (Gibco, Life Technologies). Then, the dishes were incubated with blocking solution (PBS, 5% FBS, 0.1% Triton™ X-100; Sigma-Aldrich) for 1 h at room temperature (RT). After removal of the blocking solution, the dishes were incubated with monoclonal mouse anti-β-tubulin-Cy3 antibody (Sigma-Aldrich) at a 1:100 dilution for 1 h at RT. After incubation with the antibody, the dishes were washed twice with a washing solution (PBS, 0.1% Triton X-100) and Hoechst 33258 (Sigma-Aldrich) was added and incubated for 15 min at a concentration of 2 µg/ml to allow observation of the cell nuclei. The dishes were observed under a Nikon fluorescence microscope (Nikon Eclipse TE2000-E, Tokyo, Japan).

RNA Extraction and Real-Time RT-PCR

Total RNA was extracted from tenocytes at passages 2 and 10, after 4 days (96 h) of PRP treatment, using a High Pure RNA Isolation Kit (Roche), following manufacturer's instructions. RNA concentrations were measured using a NanoDrop 2000 spectrophotometer (Thermo Scientific, Waltham, Mass., USA). One microgram of RNA was reverse-transcribed to cDNA using random hexamers in a total volume of 20 µl (SuperScript® III First-Strand Synthesis System; Invitrogen, Life Technologies).

For the real-time PCR, cDNA from each sample was diluted 5 times and 2 µl of cDNA (20 ng) was mixed with Power SYBR® Green PCR Master Mix (Applied Biosystems, Life Technologies) and 5 pmol of primers for a 20-µl final volume. Real-time PCR reactions were performed on an ABI-7900 system (Applied Biosystems, Life Technologies). The PCR reactions for each sample were performed in triplicate.

We assessed several transcription factors, including scleraxis (SCX) and Mohawk homeobox (MKX). Additionally, we evaluated the expression of matrix proteins including type 1 collagen (COL1A1), type 3 collagen (COL3A1), tenomodulin (TNMD), decorin (DCN), fibromodulin (FMOD), FN, cartilage oligomeric matrix protein (COMP), and hyaluronan synthase 2 (HAS2), the enzyme for hyaluronan (HA) synthesis. Further details, including the primer sequences and PCR conditions, are provided in table 1.

Relative expression levels were normalized to the average expression of glyceraldehyde-3-phosphate dehydrogenase (GAPDH) and TATA-box-binding protein (TBP), which were both stably expressed. Gene expression data were calculated using the $2^{-\Delta Ct}$ method.

Table 1. Primers and PCR conditions

Gene name	Primer sequence (5′–3′)	Primer sequence (3′–5′)
GAPDH	GCATTGCCCTCAACGACCACT	CCATGAGGTCCACCACCCTGT
TBP	TGCACAGGAGCCAAGAGTGAA	CACATCACAGCTCCCCACCA
COL1A1	GGCAACAGCCGCTTCACCTAC	GCGGGAGGACTTGGTGGTTTT
COL3A1	CACGGAAACACTGGTGGACAGATT	ATGCCAGCTGCACATCAAGGAC
FN	TTTGCTCCTGCACATGCTTT	TAGTGCCTTCGGGACTGGGTTC
ACAN	ACAGCTGGGGACATTAGTGG	GTGGAATGCAGAGGTGGTTT
VCAN	TGGAATGATGTTCCCTGCAA	AAGGTCTTGGCATTTTCTACAACAG
DCN	GGTGGGCTGGCAGAGCATAAGT	TGTCCAGGTGGGCAGAAGTCA
HAS2	GTCCCGGTGAGACAGATGAG	ATGAGGCTGGGTCAAGCATAG
COMP	CCGACAGCAACGTGGTCTT	CAGGTTGGCCCAGATGATG
FMOD	CAGTCAACACCAACCTGGAGAACC	TGCAGAAGCTGCTGATGGAGAA
ITGA2	TGGAATCCTTTTGCTGTTAGCTCTGG	CAGCTACTGAGCTCTGTGGTCTCATC
ITGA5	CTGTGGGGTGGCCTTCGGTTT	CGTCGCTTTGCGAGTTGTTGAG
ITGA11	CTCAGACGGTAGCATTGAGTGTGTG	GCTGAACTCAAAATCAAGACGGAAAG
ITGB1	GGATATTACTCAGATCCAACCACAGCA	TCAATGGGATAGTCTTCAGCTCTCTTG
SCX	CAGCCCAAACAGATCTGCACCTT	CTGTCTTTCTGTCGCGGTCCTT
MKX	CATCGTCATCAGAACTGAAGGCA	TCTGTTAGCTGCGCTTTCACCC
TNMD	GAAGCGGAAATGGCACTGATGA	TGAAGACCCACGAAGTAGATGCCA

Angiogenesis Protein Array

In order to examine whether the culture system (3D hydrogels vs. conventional 2D cultures) influences the angiogenic response of tendon cells to PRP, we performed an initial screening using a semiquantitative, sandwich-based glass slide antibody array (RayBio® Human Angiogenesis Antibody Array G-Series 1000, catalog No. AAH-ANG-G1; RayBiotech Inc., Norcross, Ga., USA). The array was performed according to the manufacturer's instructions and the results were normalized against positive controls. To account for any biological variability, samples from 2 cell donors and 4 PRP donors were pooled after 4 days of cultivation with PRP, in 2D cultures and 3D hydrogels independently. After centrifugation, the supernatants were harvested and stored at –20°C for protein analysis. To further confirm protein secretion, we evaluated interleukin (IL)-6, IL-8, MCP-1, and vascular endothelial growth factor (VEGF).

Quantification of Cytokines in Cell Supernatants

The reagents for ELISA assessments, including VEGF, MCP-1, IL-6, and IL-8, were purchased from PeproTech House (London, UK). SureBlue™ TMB Microwell peroxidase was purchased from KPL (Gaithersburg, Md., USA). In order to ascertain protein secretion by tendon cells, the proteins present in PRP were quantified first and subtracted from the total protein present in the conditioned media. The secreted proteins for each set of triplicates were normalized by XTT at 96 h (metabolic activity for each particular culture, cell donor/PRP donor at 96 h) [Yoshida and Murray, 2013].

Statistics

Values are expressed as means ± SE and 95% CI of technical triplicates of 8 independent cultures. ANOVA was used to compare doubling times in 2D versus 3D cultures. Comparisons of gene expression between 2D and 3D cultures were performed using the Mann-Whitney U test. Correlations were calculated using the Spearman coefficient. $p < 0.05$ was considered statistically significant. Data were analyzed using SPSS for Windows, version 18.0 (SPSS Inc., Chicago, Ill., USA).

Results

Tendon Cells in 3D PRP Hydrogels

Tendon Cells Have Similar Doubling Times in 2D Cultures and 3D Hydrogels

At passage 2, the time needed for cell duplication was similar in tendon cells cultured in 2D cultures and cells in 3D PRP hydrogels. The mean doubling time at 72 h for cells in 2D cultures was 39.98 h (SE 2.20; 95% CI 34.8–45.2), and the mean doubling time for cells in 3D hydrogels was 42.18 h (SE 1.92; 95% CI 37.6–46.7).

The PRP donor did not affect the rate of cell proliferation ($p = 0.589$), but proliferation differed between both cell donors ($p = 0.001$). These differences were corroborated in cells cultured in 2D with 10% FBS; the doubling time was 41.5 h for cell donor 1 and 51.7 h for cell donor 2.

Tendon Cell Morphology and Organization Is Different in 2D Cultures and 3D PRP Hydrogels

The cell shape and distribution in conventional 2D cultures and in 3D PRP hydrogels are shown in figure 2. Differences in the overall 'topography' of the culture and

Table 2. Tendon cell markers

Tendon cell marker	2D	3D	p
SCX, passage 2	0.075±0.029 (0.005 to 0.144)	0.212±0.060 (0.071 to 0.354)	0.012
SCX, passage 10	0.030±0.016 (–0.008 to 0.069)	0.183±0.060 (0.036 to 0.329)	0.010
MKX, passage 2	0.052±0.014 (0.020 to 0.084)	0.011±0.005 (–0.001 to 0.024)	0.028
MKX, passage 10	0.071±0.016 (0.032 to 0.11)	0.028±0.004 0.017 to 0.039	0.315
TNMD, passage 2	0.0001±0.0001 (–0.0002 to 0.0005)	0.914±0.469 (–0.196 to 2.023)	<0.001
TNMD, passage 10	0.0009±0.0007 (–0.0008 to 0.0027)	0.54±0.17 (0.12 to 0.96)	0.015

Values are presented as means ± SE (95% CI) unless otherwise stated.

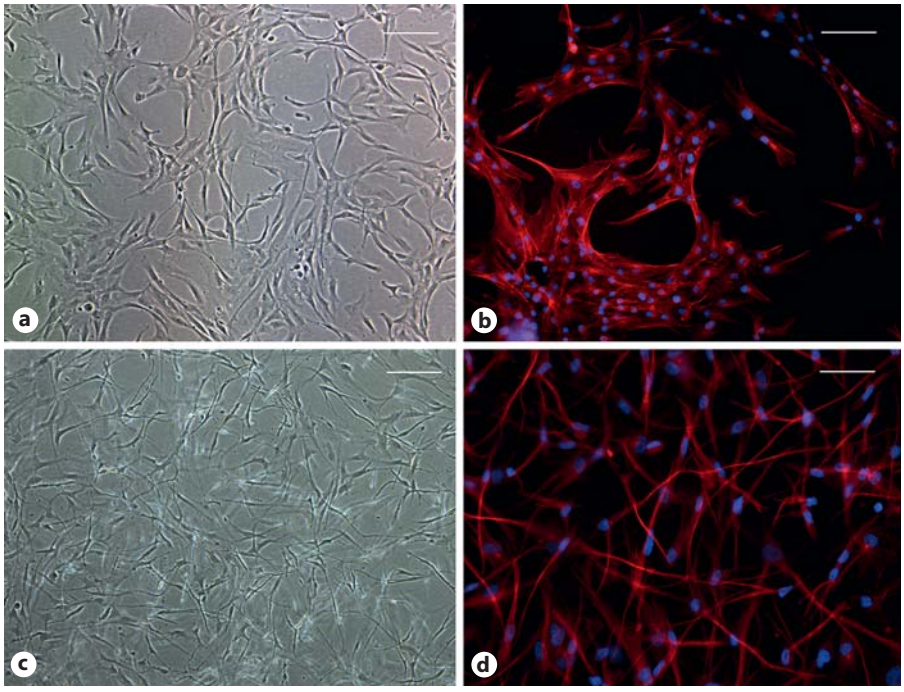

Fig. 2. a, **b** After a 4-day exposure to 10% PRP in 2D conditions, cells adopt a sheet-like organization. **c**, **d** After 4 days in 3D PRP hydrogel, extensive intercellular contacts, and cellular interactions, can be observed. Scale bars = 20 μm.

the organization of the tendon cells can be observed. Cells grown in 2D cultures, using PRP as the medium supplement, adopt a sheet-like configuration and a peculiar organization following a rattan-like structure. Interestingly, the organization in 3D PRP hydrogels is more homogenous, with cells showing a more elongated morphology with very long filiform pseudopodia extending in the 3 planes and establishing contacts with distant cells.

The Expression of TNMD and SCX Is Enhanced in 3D PRP Hydrogels

SCX was expressed at low levels in 2D cultures, but its expression increased significantly when the cells were in a 3D hydrogel environment (p = 0.012), suggesting that the physical cues detected in the 3D configuration reinforce the tenogenic identity of cells. In the same manner, the expression of the glycoprotein TNMD by native ten-

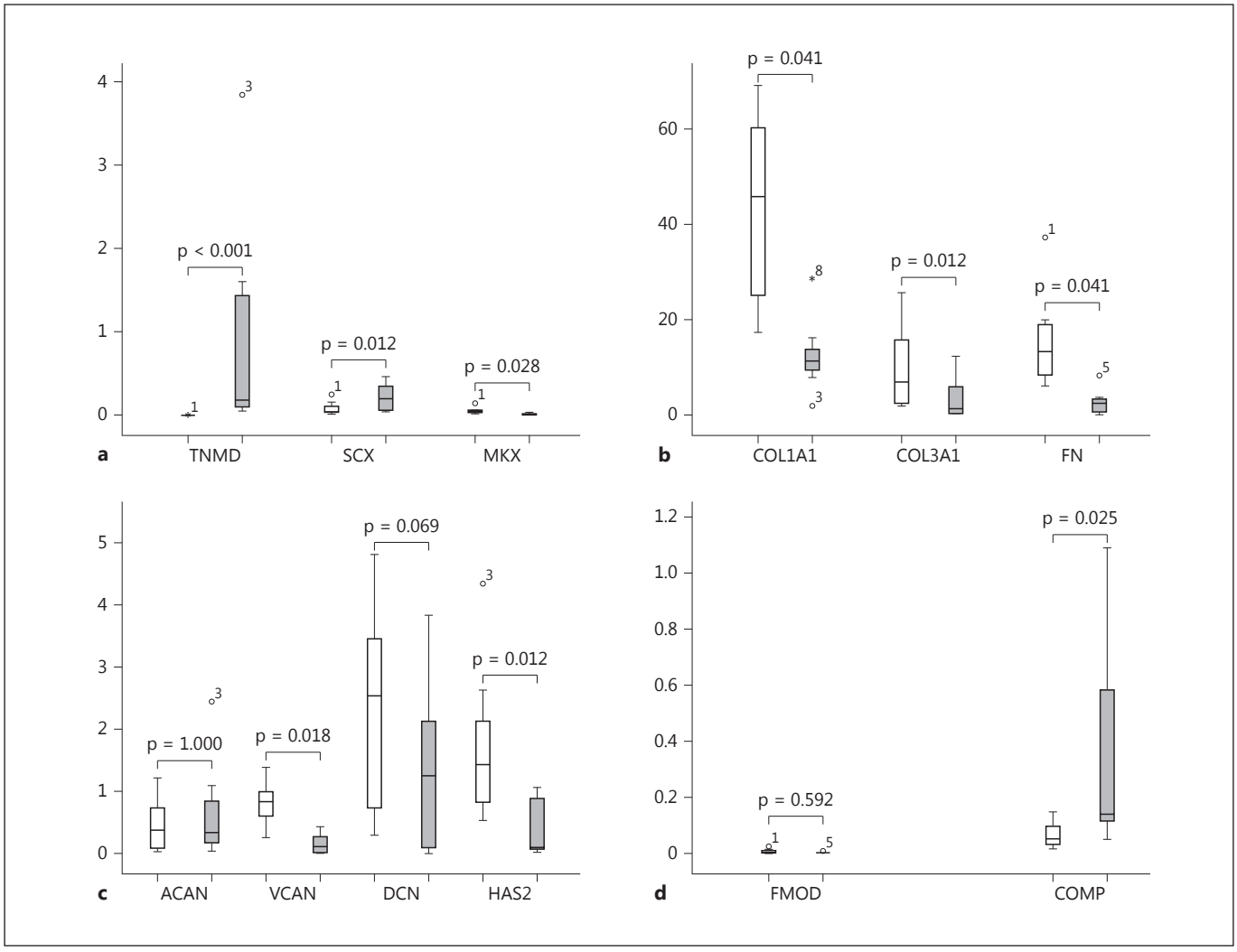

Fig. 3. The spatial configuration of tendon-derived cells modifies their transcriptional activities. **a** Critical regulators of tenogenic identity are changed. **b** The 3D configuration of tendon cells causes downregulation of the expression of the main components of the ECM. **c** Proteoglycan transcription in 3D hydrogel cultures is altered. **d** COMP expression is upregulated in 3D hydrogels. Asterisks represent extreme values >1.5 times the inter-quartile range; circles represent outliers <1.5 times the inter-quartile range.

don cells was increased in 3D PRP hydrogel environments ($p < 0.001$). Conversely, MKX showed a higher gene expression in 2D cultures than in 3D PRP hydrogels ($p = 0.028$; fig. 3a).

High-Passage Cell Culture Does Not Affect the Expression of TNMD and SCX in 3D Culture

The passage number affects cell physiology and therefore experiments are generally performed with low-passage cell cultures. We explored whether serial passaging (up to 10 passages) results in the loss of tenogenic markers (MKX, TNMD, and SCX). Remarkably, after the 10th passage, the expression levels of both SCX and TNMD were much higher in cells that were loaded in 3D PRP hydrogels compared to those in 2D cultures ($p = 0.010$ and $p = 0.015$, respectively). Detailed results are shown in table 2.

The Expression of COL1A1, COL3A1, FN, Versican, and HA Synthase 2 Is Reduced in 3D Hydrogels Compared to 2D Cultures

At 96 h, there was a significant decrease in the expression of the main molecules of tendon ECM COL1A1, COL3A1, and FN in 3D hydrogels ($p = 0.041$, $p = 0.012$,

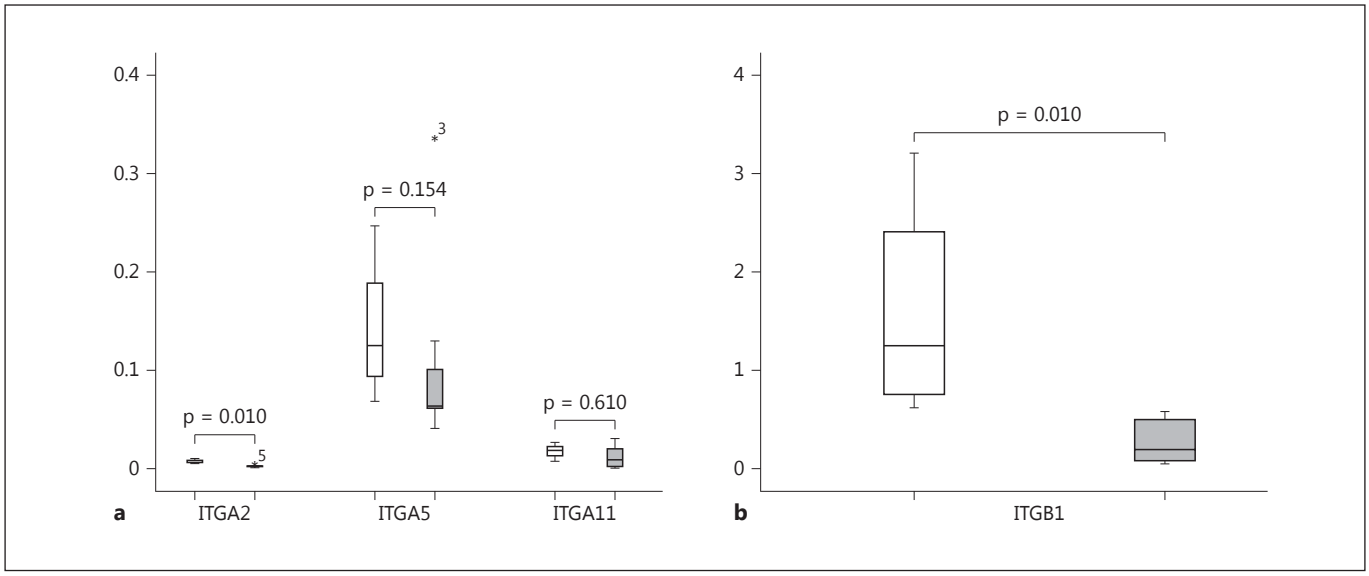

Fig. 4. Gene expression of integrin subunits in 2D cultures and 3D hydrogels: integrin subunits α_2, α_5, and α_{11} (**a**) and the β_1 integrin subunit (**b**). Asterisks represent extreme values >1.5 times the inter-quartile range.

and p = 0.041, respectively; fig. 3b). The expression of the proteoglycans aggrecan (ACAN) and DCN was similar in both culture types (p = 1.00 and p = 0.069). There was a decrease in molecules related to cell mobility, including versican (VCAN; p = 0.018) and an enzyme responsible for the synthesis of HA, i.e. HAS2 (p = 0.012; fig. 3c). FMOD showed similar low-level expression in both culture conditions, but there was an increase in COMP expression in 3D hydrogels (p = 0.025; fig. 3d). Details are shown in table 3.

In 3D hydrogels, strong correlations were found between VCAN and DCN ($\rho = 1$, $p < 0.0001$), VCAN and COL3A1 ($\rho = 1$, $p < 0.0001$), and DCN and COL3A1 ($\rho = 1$, $p < 0.0001$). DCN correlated with COL1A1 ($\rho = 0.953$, $p = 0.005$). In addition, there was a positive correlation between COL1A1 and COL3A1 ($\rho = 0.943$, $p = 0.005$). TNMD showed a strong correlation with ACAN ($\rho = 1$, $p < 0.0001$) and also with COMP ($\rho = 0.886$, $p = 0.019$); the latter correlated negatively with FMOD ($\rho = -0.886$, $p = 0.019$). FMOD also showed moderate correlations with COL1A1 ($\rho = 0.829$, $p = 0.042$) and with HAS2 ($\rho = 0.812$, $p = 0.050$). These correlations were not detected in 2D cultures. Instead, there was a negative correlation between HAS2 and VCAN ($\rho = -0.821$, $p = 0.023$) and HAS2 and COL3A1 ($\rho = -0.857$, $p = 0.014$). VCAN and SCX showed a negative correlation ($\rho = -0.757$, $p = 0.049$). Moreover, there was a positive correlation between ACAN and DCN ($\rho = 0.786$, $p = 0.036$).

Table 3. Expression of ECM molecules

ECM gene expression	2D	3D	p
COL1A1	43.6±7.1 (26.9 to 60.3)	12.6±3.1* (5.0 to 20.3)	0.041
COL3A1	9.7±3.1 (2.4 to 17.0)	3.5±1.6* (–0.3 to 7.2)	0.012
FN	15.6±3.6 (7.2 to 24.0)	2.7±1.1* (0.07 to 5.3)	0.041
ACAN	0.456±0.151 (0.097 to 0.813)	0.647±0.282 (–0.019 to 1.313)	1.00
VCAN	0.811±0.124 (0.517 to 1.103)	0.157±0.067* (–0.007 to 0.321)	0.018
DCN	2.318±0.585 (0.934 to 3.702)	1.36±0.544 (0.272 to 2.692)	0.069
HAS2	1.707±0.444 (0.656 to 2.757)	0.397±0.163 (0.129 to 0.782)	0.132
COMP	0.066±0.169 (0.026 to 0.106)	0.383±0.161 (–2.4 to 2.25)	0.545
FMOD	0.007±0.003 (0.000 to 0.014)	0.003±0.001 (0.000 to 0.005)	0.592

Values are presented as means ± SE (95% CI) unless otherwise stated. * Statistically significant.

Table 4. Expression of integrins

Integrin	2D	3D	p
ITGA2	0.005±0.000 (0.042 to 0.064)	0.002±0.000* (0.001 to 0.003)	0.010
ITGA5	0.141±0.038 (0.021 to 0.261)	0.109±0.039 (0.013 to 0.215)	0.154
ITGA11	0.013±0.006 (–0.059 to 0.084)	0.020±0.010 (–0.110 to 0.151)	0.610
ITGB1	0.751±0.132 (–0.929 to 2.432)	0.296±0.207* (–2.335 to 2.927)	0.010

Values are presented as means ± SE (95% CI) unless otherwise stated. * Statistically significant.

Expression of the α_2 and β_1 Integrin Subunits Is Reduced in 3D PRP Hydrogels

We explored whether the expression pattern of the main integrin subunits for COL1A1 and FN differed between cells in 2D cultures and in 3D PRP hydrogels. There were no differences in the expression of ITGA5 or ITGA11 (α_5 and α_{11} subunits). Instead, the subunits α_2 and β_1 specific for COL1A1 (encoded by ITGFA2 and ITGB1) were significantly decreased in 3D hydrogels ($p = 0.010$ for both integrin subunits; fig. 4a, b). Details are shown in table 4.

Secretion of Angiogenic Proteins into the Culture Media

Protein array screening technology identified several angiogenic/inflammatory proteins in the conditioned media (fig. 5). Subsequent quantification by means of ELISA revealed higher concentrations of IL-6 ($p = 0.001$) and IL-8 ($p < 0.001$) in 3D hydrogels, while MCP-1 and VEGF remained similar ($p = 0.065$ and $p = 0.878$, respectively; fig. 6).

Discussion

Experimental data on cell cultures support the use of PRP to enhance tendon healing because of its mitogenic potential and its capacity to stimulate the synthesis of ECM molecules [Anitua et al., 2005–2007]. However, this information is not completely in accordance with previously reported clinical outcomes after PRP application in tendon disorders [Andia et al., 2014a]. Given the complexity of in vivo microenvironments, it is necessary to assess the influence of PRP on tendon cell biology in a more physiologically relevant way. We developed a 3D PRP culture model and examined how it differs from classical 2D cultures.

Platelets release a pool of small diffusible molecules including growth factors, IL, and other cytokines. PRP contains, among others, relevant concentrations of IGF-1, TGF-β_1, and PDGF-BB, crucial growth factors associated with tendon tissue regeneration [Schneider et al., 2011]. Remarkably, the mitotic potential of this molecular pool is maintained when cells are cultured in 3D PRP hydrogels, indicating that signaling proteins in PRP are spatially disseminated through the hydrogel. In addition, 3D PRP hydrogels modulate the tendon cell shape and enhance the expression of some tenogenic markers.

What defines a tenocyte apart from its anatomical location is still being debated. Moreover, the lack of specific tendon biomarkers hinders the identification of possible tenocyte subsets. Currently, tendon cells are recognized based on simultaneous identification of the expression of a panel of nonspecific transcription factors, including SCX and Mohawk, and ECM molecules such as COL1A1 and COL3A1, FN, TNMD, and DCN [Nourissat et al., 2015]. In 3D PRP hydrogels, we found higher expression levels of the transcription factor SCX and the transmembrane glycoprotein TNMD, both of key importance for tendon formation and maintenance of the tenocyte phenotype. This is relevant because tendon-derived cells show signs of phenotypic drift (loss of expression of SCX and TNMD) after the first 3 passages in 2D cultures [Mazzocca et al., 2012].

Increased expression of some tendon markers, e.g. SCX, TNMD, and DCN, has been reported in the presence of IGF-1 and TGF-β_3 in 2D cultures [Qiu et al., 2013]. Interestingly, in our experimental conditions, expression of SCX and TNMD could be regained not only at low passages (e.g. 2) but also at high passages (e.g. 10), indicating that the 3D cell configuration per se can enhance the expression of these tendon-associated markers. Likewise, culturing of tendon cells in collagen scaffolds covered with fibrin led to enhanced TNMD expression [Pawelec et al., 2015].

An elongated morphology is essential in order for tenocytes to keep their phenotype and, most likely, their function [Zhu et al., 2010]. The expression levels of several ECM proteins including collagens, glycosaminoglycans, and essential integrins, are modulated by the extent of cell attachment.

Tendon repair is attributed to several concomitant mechanisms. Foremost, true tendon regeneration is

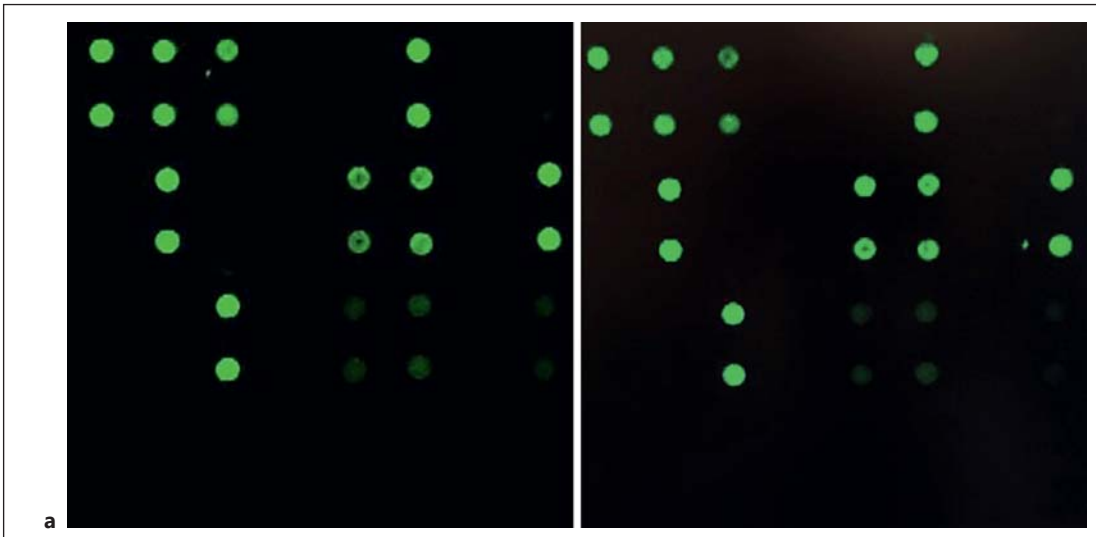

a

POS-1	POS-2	POS-3	NEG	NEG	Angiogenin	EGF	ENA-78
POS-1	POS-2	POS-3	NEG	NEG	Angiogenin	EGF	ENA-78
bFGF	GRO	IFN-γ	IGF-1	IL-6	IL-8	Leptin	MCP-1
bFGF	GRO	IFN-γ	IGF-1	IL-6	IL-8	Leptin	MCP-1
PDGF-BB	PIGF	RANTES	TGF-β_1	TIMP-1	TIMP-2	Thrombopoietin	VEGF
PDGF-BB	PIGF	RANTES	TGF-β_1	TIMP-1	TIMP-2	Thrombopoietin	VEGF
VEGF-D	NEG	NEG	NEG	NEG	NEG	NEG	NEG
VEGF-D	NEG	NEG	NEG	NEG	NEG	NEG	NEG

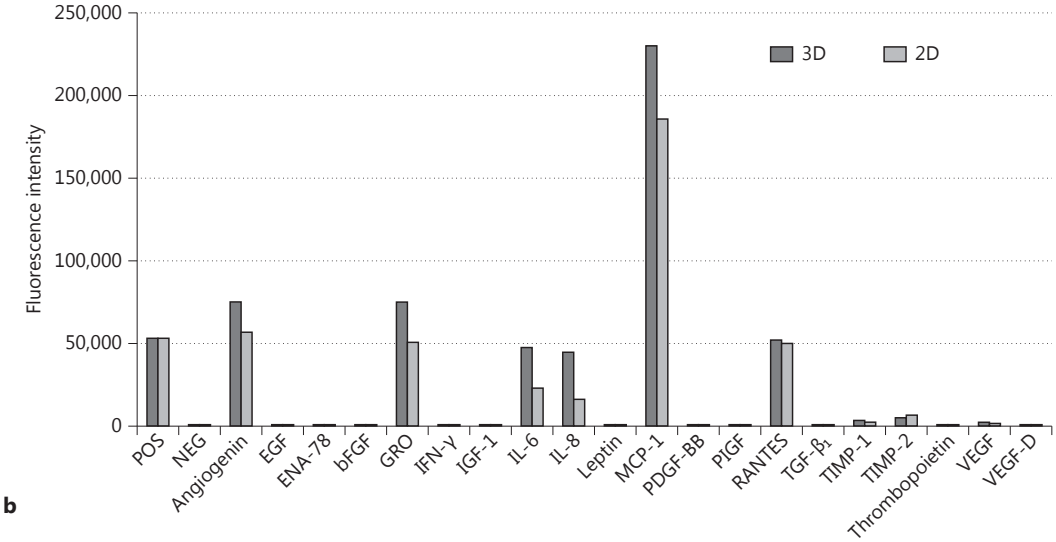

b

Fig. 5. Glass-based protein arrays for angiogenesis. **a** Representative images of antibody array profiling of proteins in 3D PRP hydrogels and 2D cultures. **b** Relative expression of angiogenic proteins in 2D cultures (light grey) and 3D PRP hydrogels (dark grey).

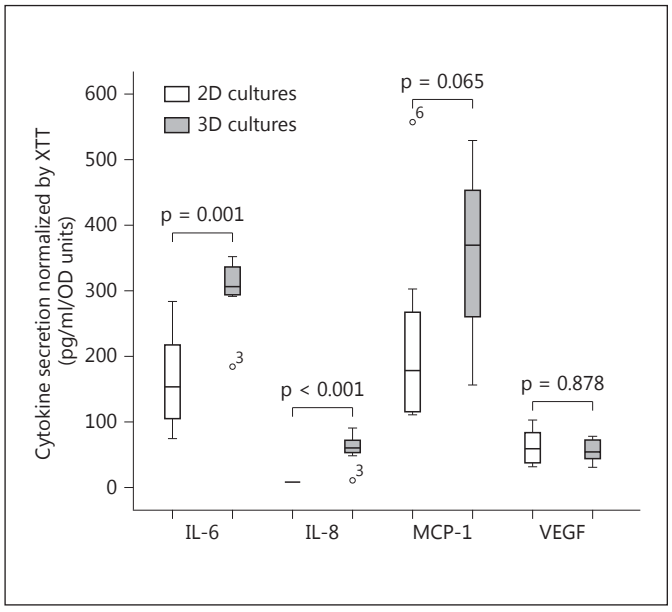

Fig. 6. Quantification of the angiogenic/inflammatory proteins present in the conditioned media of cells cultured in 3D PRP hydrogels and 2D conventional PRP-supplemented cultures. OD = Optical density. Circles represent outliers <1.5 times the interquartile range.

thought to recapitulate developmental processes, involving cell differentiation and fibrillogenesis, with restoration of native tissue properties. In vitro research in 3D fibrin constructs has proven that mature tendon cells are able to recapitulate fibrillogenesis [Bayer et al., 2014]. These results suggest that regenerative deficits in mature tendons are not associated with tendon capabilities but are related to the hostile molecular environment. Actually, differential healing responses between embryonic and adult tendons are attributed to inflammation [Glass et al., 2014]. In this regard, we revealed that inflammatory and angiogenic processes induced by PRP-intrinsic cues involve the secretion of IL-6, IL-8, MCP-1, and VEGF by tendon cells [Andia et al., 2015]. Because of their pleiotropic properties, the role of these proteins remains controversial in both physiology and pathology.

The regenerative deficits of tendons, in particular the weak response to injury, can be attributed to an intrinsic deficiency in harm detection. This failure may be due to the absence of molecular signals. In this sense, PRP provides a pool of molecular injury-related signals that help tendons to overcome this limitation. These signals are spatially propagated through the tissue to activate the healing response of cells.

In previous studies, we and other researchers have reported the angiogenic and inflammatory response of tendon cells to PRP signals [Anitua et al. 2007; Andia et al., 2015]. To verify whether the inflammatory and angiogenic paracrine effects of PRP are maintained in 3D conditions, we performed specific glass-based proteomic arrays for angiogenesis. Our analysis revealed a few differences between 2D and 3D cultures, but the secretion of major angiogenic/inflammatory cytokines remained unaffected, indicating that 2D culture does not modify the inflammatory and angiogenic response of tendon cells to PRP-secreted molecules.

This study has several limitations. Tendon cells show different patterns of gene expression when cultured in PRP hydrogels. However, gene expression is a highly dynamic process that needs multiple assessments at different time points in order to be fully characterized. Regarding protein expression, longer culture times can provide a more complete picture of fibrillogenesis as well as the angiogenic/inflammatory effects of PRP.

Meaningless information/data derived from experimental in vitro studies may be an obstacle to the successful development of PRP-augmented regenerative therapies. In this context, we have shown how cells behave when cultured in 3D PRP hydrogels in contrast to 2D cultures. Future studies using molecular crowding strategies, mechanical stimulation, and hypoxia in the presence of PRP are needed in order to mimic more physiological environments in tendons.

Although experimental research cannot substitute clinical research, we believe that improving in vitro models may help to understand how PRP influences tendon cell biology and to provide information that can be applied to improve PRP therapies and the design of clinical trials.

Acknowledgments

This work was partially supported by Gaitek, Departamento de Desarrollo Económico y Competitividad, Gobierno Vasco.

Disclosure Statement

The authors declare that they have no conflicts of interest.

References

Andia, I., P.M. Latorre, M.C. Gomez, N. Burgos-Alonso, M. Abate, N. Maffulli (2014a) Platelet-rich plasma in the conservative treatment of painful tendinopathy: a systematic review and meta-analysis of controlled studies. Br Med Bull *110:* 99–115.

Andia, I., E. Rubio, N. Maffulli (2015) Platelet-rich plasma modulates the secretion of inflammatory/angiogenic proteins by inflamed tenocytes. Clin Orthop Relat Res *473:* 1624–1634.

Andia, I., E. Rubio-Azpeitia, N. Maffulli (2014b) Hyperuricemic PRP in tendon cells. Biomed Res Int *2014:* 926481.

Andia, I., M. Sanchez, N. Maffulli (2010) Tendon healing and platelet-rich plasma therapies. Expert Opin Biol Ther *10:* 1415–1426.

Anitua, E., I. Andia, M. Sanchez, J. Azofra, M. del Mar Zalduendo, M. de la Fuente, P. Nurden, A.T. Nurden (2005) Autologous preparations rich in growth factors promote proliferation and induce VEGF and HGF production by human tendon cells in culture. J Orthop Res *23:* 281–286.

Anitua, E., M. Sanchez, A.T. Nurden, M. Zalduendo, M. de la Fuente, J. Azofra, I. Andia (2007) Reciprocal actions of platelet-secreted TGF-beta1 on the production of VEGF and HGF by human tendon cells. Plast Reconstr Surg *119:* 950–959.

Anitua, E., M. Sanchez, A.T. Nurden, M. Zalduendo, M. de la Fuente, G. Orive, J. Azofra, I. Andia (2006) Autologous fibrin matrices: a potential source of biological mediators that modulate tendon cell activities. J Biomed Mater Res A *77:* 285–293.

Bayer, M.L., P. Schjerling, A. Herchenhan, C. Zeltz, K.M. Heinemeier, L. Christensen, M. Krogsgaard, D. Gullberg, M. Kjaer (2014) Release of tensile strain on engineered human tendon tissue disturbs cell adhesions, changes matrix architecture, and induces an inflammatory phenotype. PLoS One *9:* e86078.

Cazander, G., G.N. Jukema, P.H. Nibbering (2012) Complement activation and inhibition in wound healing. Clin Dev Immunol *2012:* 534291.

Glass, Z.A., N.R. Schiele, C.K. Kuo (2014) Informing tendon tissue engineering with embryonic development. J Biomech *47:* 1964–1968.

Hammerman, M., P. Aspenberg, P. Eliasson (2014) Microtrauma stimulates rat Achilles tendon healing via an early gene expression pattern similar to mechanical loading. J Appl Physiol *116:* 54–60.

Kovacevic, D., L.V. Gulotta, L. Ying, J.R. Ehteshami, X.H. Deng, S.A. Rodeo (2015) rh-PDGF-BB promotes early healing in a rat rotator cuff repair model. Clin Orthop Relat Res *473:* 1644–1654.

Lamplot, J.D., M. Angeline, J. Angeles, M. Beederman, E. Wagner, F. Rastegar, B. Scott, C. Skjong, D. Mass, R. Kang, S. Ho, L.L. Shi (2014) Distinct effects of platelet-rich plasma and BMP13 on rotator cuff tendon injury healing in a rat model. Am J Sports Med *42:* 2877–2887.

Mazzocca, A.D., D. Chowaniec, M.B. McCarthy, K. Beitzel, M.P. Cote, W. McKinnon, R. Arciero (2012) In vitro changes in human tenocyte cultures obtained from proximal biceps tendon: multiple passages result in changes in routine cell markers. Knee Surg Sports Traumatol Arthrosc *20:* 1666–1672.

Nourissat, G., F. Berenbaum, D. Duprez (2015) Tendon injury: from biology to tendon repair. Nat Rev Rheumatol *11:* 223–233.

Nurden, A.T., P. Nurden, M. Sanchez, I. Andia (2008) Platelets and wound healing. Front Biosci *13:* 3532–3548.

Pawelec, K.M., R.J. Wardale, S.M. Best, R.E. Cameron (2015) The effects of scaffold architecture and fibrin gel addition on tendon cell phenotype. J Mater Sci Mater Med *26:* 5349.

Qiu, Y., X. Wang, Y. Zhang, R. Rout, A.J. Carr, L. Zhu, Z. Xia, A. Sabokbar (2013) Development of a refined tenocyte differentiation culture technique for tendon tissue engineering. Cells Tissues Organs *197:* 27–36.

Schneider, P.R., C. Buhrmann, A. Mobasheri, U. Matis, M. Shakibaei (2011) Three-dimensional high-density co-culture with primary tenocytes induces tenogenic differentiation in mesenchymal stem cells. J Orthop Res *29:* 1351–1360.

Spanoudes, K., D. Gaspar, A. Pandit, C. Holladay, A. Pandit, D. Zeugolis (2014) The biophysical, biochemical, and biological toolbox for tenogenic phenotype maintenance in vitro. Trends Biotechnol *32:* 474–482.

Yoshida, R., M.M. Murray (2013) Peripheral blood mononuclear cells enhance the anabolic effects of platelet-rich plasma on anterior cruciate ligament fibroblasts. J Orthop Res *31:* 29–34.

Zhu, J., J. Li, B. Wang, W.J. Zhang, G. Zhou, Y. Cao, W. Liu (2010) The regulation of phenotype of cultured tenocytes by microgrooved surface structure. Biomaterials *31:* 6952–6958.